IEEE Access
Multidisciplinary | Rapid Review | Open Access Journal

Received March 17, 2020, accepted April 13, 2020, date of publication April 21, 2020, date of current version May 6, 2020.

Digital Object Identifier 10.1109/ACCESS.2020.2989356

Investigation of the Dielectric and Thermal Properties of Non-Edible Cottonseed Oil by Infusing h-BN Nanoparticles

RIZWAN A. FARADE[1], NOOR IZZRI BIN ABDUL WAHAB[1], (Senior Member, IEEE), DIAA-ELDIN A. MANSOUR[2], (Senior Member, IEEE), NORHAFIZ B. AZIS[1], (Senior Member, IEEE), JASRONITA JASNI[1], (Senior Member, IEEE), N. R. BANAPURMATH[3], AND MANZOORE ELAHI M. SOUDAGAR[4]

[1]Department of Electrical and Electronics Engineering, Faculty of Engineering, University Putra Malaysia, Seri Kembangan 43400, Malaysia
[2]Department of Electrical Power and Machines Engineering, Faculty of Engineering, Tanta University, Tanta 31511, Egypt
[3]Department of Mechanical Engineering, B.V.B. College of Engineering and Technology, KLE Technological University, Hubli 580031, India
[4]Department of Mechanical Engineering, Faculty of Engineering, University of Malaya, Kuala Lumpur 50603, Malaysia

Corresponding authors: Rizwan A. Farade (rizwan.projects@gmail.com) and Noor Izzri Bin Abdul Wahab (izzri@upm.edu.my)

This work was supported in part by the University Putra Malaysia under Grant GPB 9630000.

ABSTRACT Vegetable oils have emerged as insulating fluids in transformer applications and as a prominent and effective alternative for traditional dielectric fluids. However, most of vegetable oils are edible causing their application on a large scale to be limited. In the present work, a novel non-edible vegetable oil is developed as an insulating fluid. The developed oil is oxidation-inhibited cottonseed oil (CSO) based nanofluids. Tertiary butylhydroquinone was used as antioxidant. The concept of nanofluids was used to overcome the limited dielectric and thermal properties of cottonseed oil. Hexagonal Boron Nitride (h-BN) nanoparticles at low weight fractions (0.01 - 0.1 wt%) were proposed as nanofillers to achieve adequate dielectric strength and improved thermal conductivity. Stability of prepared CSO based nanofluids was analyzed using Ultraviolet–visible (UV-Vis) spectroscopy. Then, the prepared nanofluids were tested for dielectric and thermal properties under a temperature range between 45 °C and 90 °C. The dielectric properties include breakdown strengths under AC and lightning impulse voltages, dielectric constant, dissipation factor, and resistivity, while thermal properties include thermal conductivity and thermogram analysis. The dielectric and thermal properties were significantly improved in CSO based nanofluids. The creation of electric double layer at nanoparticle/oil interface and the lattice vibration of nanoparticles were used to clarify the obtained results. The proposed CSO based h-BN nanofluids open up a great opportunity in both natural ester insulating fluid applications and thermal energy management systems.

INDEX TERMS Vegetable oils, transformers, nanofluids, dielectric properties, thermal properties.

NOMENCLATURE

b	Absorbance in y intercept
BDV	Breakdown voltage [kV]
c_p	Specific heat capacity [J/(kg.K)]
CSO	Cottonseed oil
EDL	Electric Double Layer
Enh.	Enhancement
h-BN	Hexagonal Boron Nitride
k_B	Boltzmann constant [1.3806505e^{-23} J/K]
LI	Lightning impulse
m	Coefficient of molar extinction [M^{-1}.cm^{-1}]
NEIO	Natural ester insulating oil
wt%	Weight percentage
X	Concentration [mol/l or M]
Y	Absorbance

GREEKS

μ	Viscosity coefficient [kg/(m.s)]
$\varepsilon, \varepsilon_o$	Permittivity, Permittivity of space (F.m^{-1})
ε'	Dielectric constant
ε''	Loss factor
ρ	Density (g.cm^{-3})
σ	Electrical conductivity [S.m^{-1}]
τ	Relaxation time (s)
N_1, N_2 & N_3	No. of molecules of oil, nanoparticle, and oil at nanoparticle/oil interface

The associate editor coordinating the review of this manuscript and approving it for publication was Jenny Mahoney.

r	Radius [m]
RTP	Room temperature and pressure
SD	Standard Deviation
T	Temperature [°C]
TBHQ	Tertiary butylhydroquinone
λ	Thermal conductivity [W/m.K]
Φ	Volume concentration
$\alpha_1, \alpha_1 \& \alpha_1$	Polarizability of N_1, N_2, and N_3

SUBSCRIPTS

p	Particle
f	Fluid
nf	Nanofluid

I. INTRODUCTION

It is important to maintain the key properties of insulating fluids used in transformers. These fluids have dual roles, where they perform as an electrical insulator and heat transfer agent. The dielectric strength of these fluids should be adequate to withstand the potential range of electrical stress imposed during service. On the other hand, combinations of their viscosity, thermal conductivity, and specific heat should be sufficient to transfer heat from transformer to surroundings. In addition, insulating fluids should have a sufficiently high flash point and fire point to meet safety standards. Finally, they should be resistant to oxidation and deterioration.

Owing to sustainability, biodegradability and pollution-free nature of natural ester insulation oils, many researchers and industries investigated such oils for transformer applications [1]–[3]. As a result, several international standards were devoted to these oils such as ASTM D6871, IEC 62770, IEEE C57.155-2014, ASTM D6871, IEEE C57.147-2018, and IEC 63012. These standards endorse modified and blended NEIOs in transformers, assist equipment manufacturers and service companies to determine the suitability of unused NEIOs received from suppliers, and assist transformer operators in assessing and maintaining NEIOs in a serviceable condition.

Turning vegetable oil feedstock into a competitive commercial transformer grade isolating oil with better inherent properties imposes numerous practical consequences and challenges. The first challenge is the oxidation tendency of vegetable oils with corresponding aging and impact on various oil properties [4]. The second and important challenge is the dependence of vegetable oils on edible products. Accordingly, this paper aims to develop a novel non-edible vegetable oil as an insulating fluid.

In India, agro-technological innovation and biotechnology offers tremendous potential for sustainable and cost-effective production of cotton [5], whereas cottonseed oil is not as common as edible oil. On the other side, CSO oil is biodegradable and non-toxic making it an environmentally friendly fluid. In addition, it has high flash point and fire point [6]. Despite CSO has these favorable characteristics, it has a high level of un-saturated fatty acid, leading to a greater risk of oxidation. However, to resolve this limitation, the base feedstock can be upgraded to higher oleic content by means of genetically modified CSO [7] or by using antioxidant additives.

Blending and dispersing stable ultra-fine nanoparticles, such as metals, oxides, nitrides, carbide ceramics, and carbon nanotubes, into fluids forms what is called nanofluids. These nanofluids had several distinct characteristics, including dielectric and thermal characteristics [8]–[12]. Nanoparticles can be classified into conductors, semiconductors, and insulators. The high surface area of two-dimensional materials leads to an efficient heat transfer phenomenon and is a better alternative for the application with nanofluids. The h-BN or graphene nanoparticles have a multifaceted feature among various 2D materials. However, h-BN overtakes other nanofillers and is an enticing material with high thermal conductivity and electrical insulation properties [13], [14]. Furthermore, theoretical studies demonstrate that the planes of h-BN can achieve high thermal conductivity [15]. Table 1 shows, few previous experimental studies on nano-infused natural esters. These studies show that there is a considerable percentage enhancement in the electro-thermal characteristics of nanofluids compare to corresponding base fluids.

In the present investigation, it is aimed to develop non-edible CSO as natural ester insulating fluids through inclusion of antioxidant and filling with h-BN nanofillers. Inclusion of antioxidant will enable to resist the oxidation process of the oil, while filling with h-BN nanofillers will enable to enhance the dielectric and thermal properties of the oil. Tertiary butylhydroquinone (TBHQ) has been used as antioxidant. Four dosage levels (0.01, 0.02, 0.05, and 0.1 wt%) of h-BN nanoadditives have been introduced into base TBHQ cottonseed oil. Comprehensive overview on synthesis, characterization and stability analysis of CSO based h-BN nanofluids is presented. Breakdown strengths under AC and lightning impulse voltages are evaluated. Also, other dielectric properties such as dielectric constant, dissipation factor, and resistivity are measured. In addition, thermal properties including thermal conductivity and thermogram analysis are obtained. All these results are compared to that of the base CSO. Finally, physical mechanisms behind the obtained results are discussed considering the effects of 2D material (h-BN) and the role of electric double layer at nanoparticle/oil interface.

II. MATERIALS AND METHODOLOGY

The h-BN nanoparticles were procured from Intelligent Materials Pvt. Ltd. (NANOSHEL Stock No: NS6130-02-260 CAS: 10043-11-5). The characteristics of the obtained h-BN nanoparticles are as follows. The size of the h-BN nanoparticles is in the range of 50-70 nm, Young's modulus of 14-60 GPa, and a density of 2.29 g/cm^3. The h-BN nanofluids were prepared using the below mentioned process with various weight percentages, 0.01, 0.02, 0.05, and 0.1. Fig. 1a and Fig. 1b illustrate the visualization of the powdered sample and produced nanofluids at various h-BN weight percentages, respectively.

TABLE 1. Experimental studies on nano-infused natural esters and attained percentage enhancement in the characteristics.

Authors	Base oil	Nanoparticles	Characteristics	Enh. (%)
R. Madavan et al. [13]	Honge oil	BN, 40 nm size	AC BDV at 0.5 vol %	0
	Neem oil	0.05-0.5 vol %	AC BDV at 0.5 vol %	+ 2.3
	Mustard oil		AC BDV at 0.5 vol %	+ 9.5
	Punna oil		AC BDV at 0.25 vol %	+ 9.5
R. Madavan et al. [13]	Honge oil	Al_2O_3, 30-70 nm size	AC BDV at 0.5 vol %	+ 4.7
	Neem oil	0.05-0.5 vol %	AC BDV at 0.5 vol %	+ 2.3
	Mustard oil		AC BDV at 0.25 vol %	+ 7.14
	Punna oil		AC BDV at 0.25 vol %	+9.5
R. Madavan et al. [13]	Honge oil	Fe_3O_4, 50-75 nm size	AC BDV at 0.5 vol %	+ 2.3
	Neem oil	0.05-0.5 vol %	AC BDV at 0.5 vol %	+ 2.3
	Mustard oil		AC BDV at 0.25 vol %	+ 9.5
	Punna oil		AC BDV at 0.5 vol %	+ 11.9
Wei Yao et al. [14]	FR3 vegetable oil	h-BN, 300-700 µm	AC BDV at 0.01 vol %	+ 18
		0.015-0.1 vol %	Positive LI BDV at 0.01 vol %	+ 23
			Resistivity at 0.1 vol %	+ 63
			Dissipation factor at 0.1 vol %	- 28
			Thermal conductivity at 0.1 vol %	+ 11.9
Grzybowski et al. [16]	Refined bleached deodorized rapeseed oil	Fe_3O_4, 30 nm	AC BDV at 0.004 wt %	+ 20
		0.004 wt %	Positive LI BDV at 0.004 wt %	+ 37
Jian Li et al. [17]	FR_3 vegetable oil	Fe_3O_4, 40.7 nm	AC BDV at 0.04 vol %	+ 24.5
		0.40 vol%		
Mohammed Javed et al. [18]	Waste palm oil	CuO, 25 nm size	Thermal conductivity at 0.7 wt%	+ 190
		0.1-0.9 wt %		
Ayesha Hameed et al. [19]	Kopakseed oil	MWCNT < 100 nm	Thermal conductivity at 0.1 wt %	+ 6.15
		0.1 wt %		

Two-step method was implemented for preparing nanofluids in the context of its advantages compared to one-step method, where it has lower cost, more productivity, and reduced particle waste. CSO was used for the present implementation as the base fluid. This vegetable oil was provided by local supplier in India from M/s S S Odunavar Industries. The TBHQ antioxidant was used as a synthetic antioxidant due to its effectiveness at high temperatures in comparison to other synthetic antioxidants [2]. It was supplied from Sigma Aldrich. A 0.02% of TBHQ was added to CSO and the solution was stirred at 80 °C for 1.5 hour with a specific interval after each 30 minutes. The addition of antioxidants suppresses the decomposing of the oil at high temperatures. The measured quantity of h-BN is then added to the solution and stirred again for 30 minutes at the same temperature. The stable dispersion is then achieved by sonication for a period of 1 hour by a probe sonicator.

The boron nitride nanosheets consists of covalently bonded hexagonal B and N (sp2–hybridization). These h-BN layers are stacked on the top of each other, where the adjacent layers are held together by a weak force of van der Waals, as shown in Fig. 1c. The h-BN nanosheets consist of mono-layered h-BN planes. The 2D h-BN nanosheets are exfoliated from bulk h-BN by long term sonication similar to the process adopted in [20]. Fig. 1d shows pictorially exfoliation of h-BN nanosheets.

III. INSTRUMENTATION OF DATA GATHERING

Scanning Electron Microscope (SEM) (JSM-IT 500) was used to show morphological visualization of the h-BN nanoparticles at various magnification levels with an acceleration voltage of 20 kV. Also, Transmission Electron Microscope (HRTEM, JEOL-JEM 2100 PLUS), operating at acceleration voltage of 200 kV, validated the size and morphological analysis of the h-BN nanoparticles. On the other hand, powder X-ray diffraction (XRD) (Philips X'pert MPD) validated phase purity detection of h-BN nanoparticles, with Cu Kß radiation in the 5-90° (2θ) range. Nanofluid stability

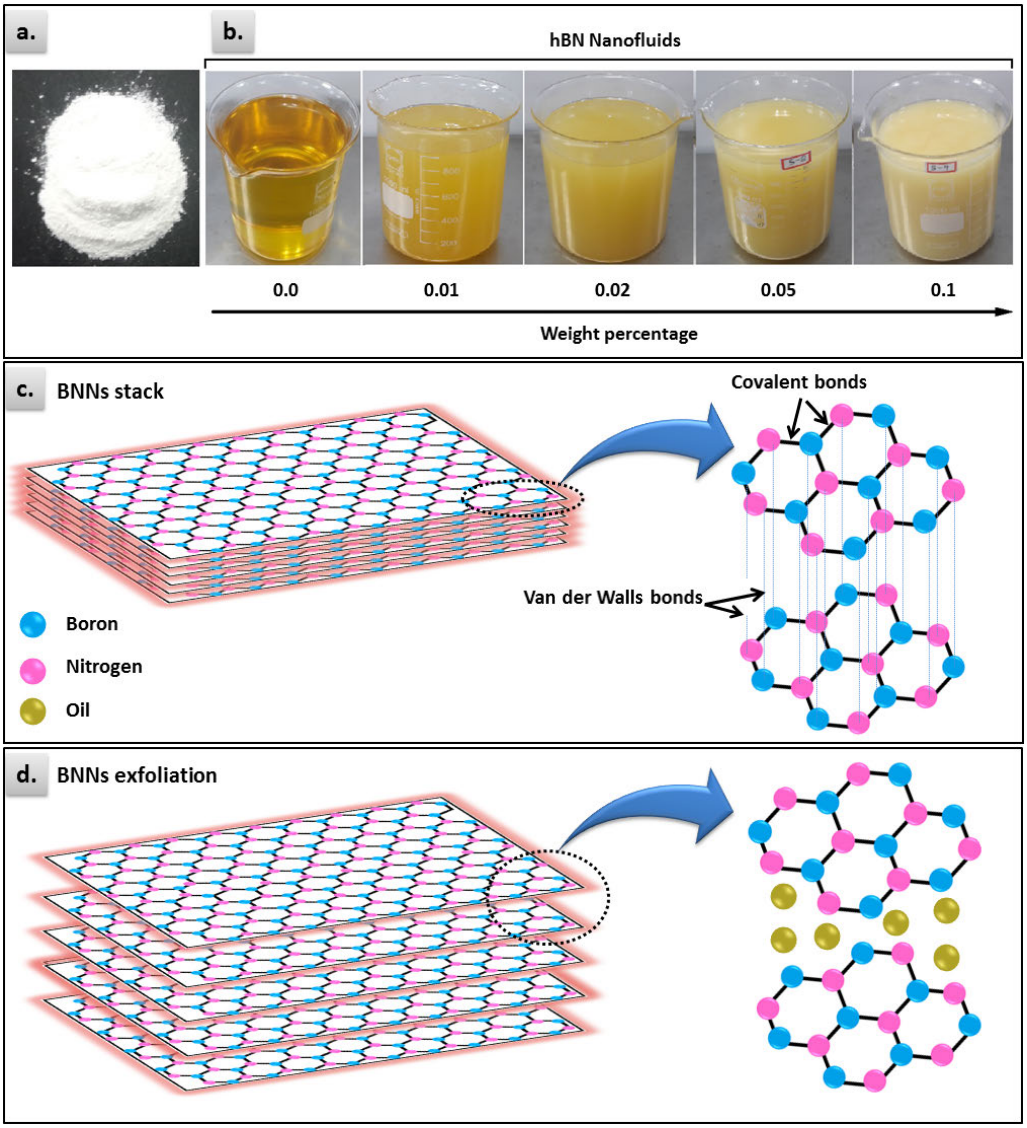

FIGURE 1. (a) h-BN powder sample visual picture (b) Prepared NFs with different h-BN loading (c) Stacked h-BN sheets before probe sonication (d) h-BN sheets exfoliation after long term probe sonication.

was measured using a UV-Vis spectrometer (Chemito Spectrascan UV-2700).

According to IEC156 and ASTM D3300 standards, the AC breakdown and impulse breakdown voltages of the prepared CSO/nanofluids were measured at room temperature. Based on these standards; electrode configurations, voltage increasing method/voltage ramp rate, time intervals, and other useful information are detailed in Table 2. ADTR instrument from ELTEL was used to measure loss tangent, dielectric constant, and resistivity of CSO/nanofluids at a standard operating frequency of 50 Hz and at four specific temperatures (45 °C, 60 °C, 75 °C, and 90 °C). For dielectric constant and loss tangent measurements, the testing voltage was set at 500 V, 50 Hz AC, while for resistivity measurements, it was set at 500 V, DC. The precision of the measurement device is ±0.1%, ±1%, and 2-5% for dielectric constant, loss tangent, and resistivity, respectively.

Thermal conductivity of CSO/nanofluids was quantified by the KD2 PRO equipment from Decagon using the transient hot-wire method. Following factory calibration, the accuracy is about ±5% for the used sensor as given in the instrument specifications. To maintain the accuracy in the test results, the used sensor is crosschecked with a standard material before testing thermal conductivity of samples. Measurements were conducted at four different temperatures, 35 °C, 45 °C, 55 °C, and 65 °C.

For further thermal conductivity verification of CSO/nanofluids, thermal response tests were conducted using the experimental setup demonstrated in Fig. 2a. In brief, 100 ml of CSO/nanofluids was put into a beaker. Then, the electric current preheats CSO/nanofluids at a certain fixed power level for 26 minutes and the specimen was allowed to cool down naturally for the next 26 minutes. The heating and cooling response were recorded. Moreover, the thermal

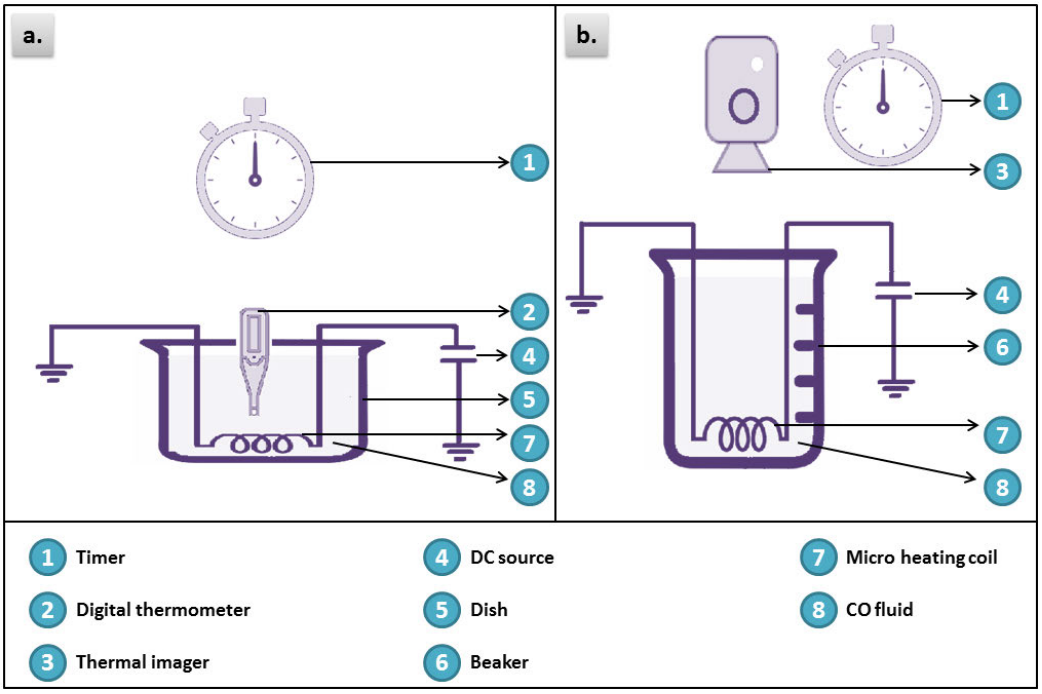

FIGURE 2. Experimental set-up of (a) Thermal response testing (b) Surface temperature imaging.

conductivity of CSO/nanofluids was validated through analyzing surface temperature images captured by the thermal imaging camera Fluke Ti125. Fig. 2b shows this experimental setup in detail. The experimental process includes heating 100 ml of various samples in a beaker under a certain fixed power level for 45 minutes and capturing surface temperature images at a specified time interval. The heating method is similar to that performed in thermal response tests.

IV. CHARACTERIZATION AND STABILITY ANALYSIS

Comprehensive characterization of h-BN nanoparticles and dispersion stability analysis of CSO nanofluids are reported in this section.

A. CHARACTERIZATION OF H-BN NANOPARTICLES

SEM samples were prepared on a carbon tape bonded on aluminum stub. A little h-BN sample was taken and placed on the carbon tape, then the loose particles were removed. After that, the stub was attached to the sample holder and put into the sample chamber for SEM analysis. Fig. 3(a-c) illustrates the SEM images of h-BN nanoparticles. From the SEM analysis, the existence of h-BN sheets at higher magnifying levels is realized, the bulk structure is verified, and irregular morphology in this structure is observed.

During TEM samples preparation, h-BN nanoparticles are dispersed in ethanol. A drop of nanoparticle solution was deposited on the copper grid and was vacuum dried at room temperature before TEM imaging. Fig. 3(d and e) show TEM-images at two magnification levels. Fig. 3f shows that each sheet consists of stacked atomic layers, where each fringe depicts one atomic layer. Selected area electron diffraction pattern is shown in Fig. 3g. The periodic spots in the figure indicate the high degree of crystallinity of h-BN, and also indicate the six-fold symmetry. The pattern of h-BN X-ray diffraction (XRD) is shown in Fig. 3h. The pattern is captured in the 2-theta (2θ) range (from 5-90°) at speed of 50° per minute with step width 0.01°. From the pattern, the peaks are obtained at 26.6°, 41.6°, 43.8°, 50.1°, 55.1°, and 75.8°, that are indexed (002), (100), (101), (102), (004), and (110), respectively, representing hexagonal phase-planes of h-BN [21], [22].

B. STABILITY ANALYSIS OF H-BN DISPERSED NANOFLUIDS

Dispersion stability is a critical issue that affects the properties of nanofluids for various applications. One of the most effective ways to evaluate nanofluid stability is spectral absorption experiments. The following equation can establish the relation between absorbance and concentration:

$$y = mx + b \tag{1}$$

The nanofluid stabilization against the concentration of nanoparticles is strongly affected by the characteristics of the suspended particles and the base fluid. The higher levels of nanoparticles in the fluid lead to an increasing number of molecules into the fluid causing agglomeration with a subsequent increase in the weight. As a result, nanoparticles settle off the suspension and become less stable. Table 3 shows the absorbance values recorded on the first day and eighth day after preparation of nanofluids. At all concentrations of

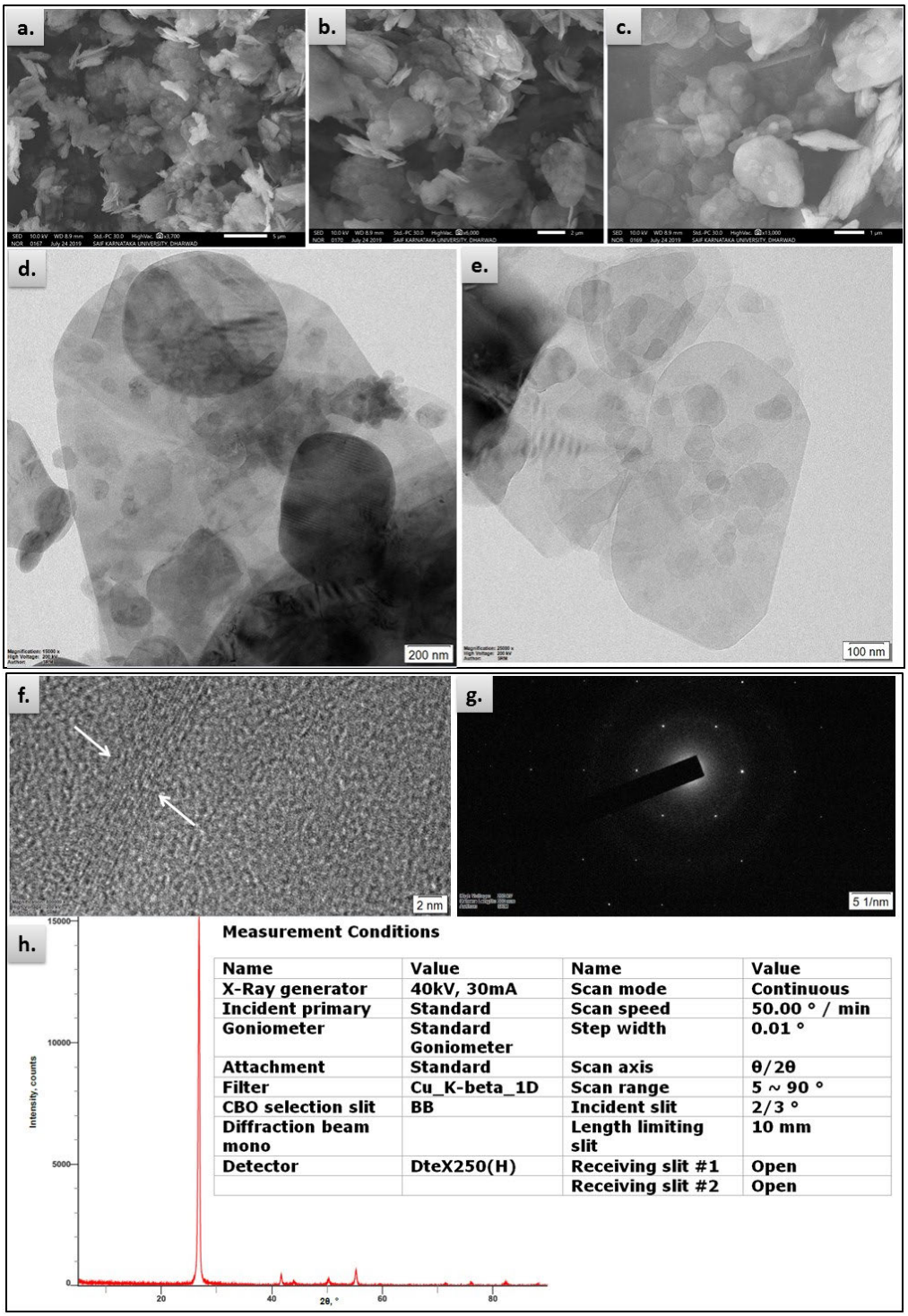

Name	Value	Name	Value
X-Ray generator	40kV, 30mA	Scan mode	Continuous
Incident primary	Standard	Scan speed	50.00 ° / min
Goniometer	Standard Goniometer	Step width	0.01 °
Attachment	Standard	Scan axis	θ/2θ
Filter	Cu_K-beta_1D	Scan range	5 ~ 90 °
CBO selection slit	BB	Incident slit	2/3 °
Diffraction beam mono		Length limiting slit	10 mm
Detector	DteX250(H)	Receiving slit #1	Open
		Receiving slit #2	Open

FIGURE 3. Characterization of h-BN nanoparticles: SEM analysis at magnification levels: a) 3700X, b) 6000X, and c) 13000X; TEM analysis at magnification levels: d) 15000X, and e) 25000X; f) The edge area of the h-BN, indicating sheet consists of a few stacked atomic layers; g) Selected area electron diffraction pattern showing six-fold symmetry; and h) XRD analysis.

h-BN nanoparticles, there is no significant reduction in the absorbance values at the eighth day comparing to the first day, maintaining stability above 95% for all samples. This indicates that CSO nanofluids are quite stable.

V. ELECTRICAL MEASUREMENTS OF CSO/h-BN DISPERSED NANOFLUIDS

Inclusive dielectric properties of CSO/nanofluids are presented in this section. These properties include breakdown

TABLE 2. Specifications of the AC and impulse breakdown test.

Property	AC breakdown test IEC 156	Impulse breakdown test ASTM D3300
Electrode type	Brass;12.5 mm diameter; sphere to sphere	Brass;12.5 mm diameter; needle to sphere
Electrode gap	2.5 mm	2.5 mm
Voltage increasing method	NA	Step by step, 3 shots per step, step voltage 5 kV
Voltage ramp rate	2 kV/s	NA
Time interval between tests/shots	60 s	60 s
Results	10 breakdowns	10 breakdowns
Impulse generator	NA	1.2µs/50µs standard lightning impulse.
Polarity	NA	Negative needle polarity

TABLE 3. Stability analysis of CSO/nanofluids with UV-Vis spectroscopy.

Weight percentage (wt%)	Absorbance		Stability (%)
	Day-1	Day-8	
0.01	2.78	2.74	98.56
0.02	6.43	6.34	98.60
0.05	12.50	12.22	97.76
0.1	24.50	23.49	95.87

strengths under AC and lightning impulse voltages (at RTP) and; dielectric constant, dissipation factor, and resistivity (at 45 °C to 90 °C).

A. BREAKDOWN STRENGTH OF CSO/NANOFLUIDS

Evaluating breakdown strengths of CSO/nanofluids is important to ensure that they can bear high voltages. AC breakdown strength of prepared samples was measured according to IEC 156 standard, whereas impulse breakdown strength was measured according to ASTM D3300 standard. The mean AC breakdown voltage for base CSO with TBHQ antioxidant was estimated as 37.6 kV. After filling with h-BN nanoparticles, an enhancement in AC breakdown voltage was achieved and attained a maximum percentage increment of 63.3% at a weight percentage of 0.1 wt%. The mean breakdown AC voltages are listed in the first half of Table 4 along with standard deviation and percentage enhancement at all weight percentages. Whereas, the mean impulse breakdown voltage for base CSO with TBHQ antioxidant was estimated as 141.2 kV, and achieved a maximum enhancement up to 5.4% at a weight percentage of 0.1 wt%. The mean breakdown impulse voltages are listed in the second half of Table 4 along with standard deviation and percentage enhancement at all weight percentages. Fig. 4a and Fig. 4b depicts the mean value and standard deviation of the AC and the impulse breakdown voltages against the weight percentages, respectively.

B. DIELECTRIC CONSTANT OF CSO/NANOFLUIDS

The dielectric constant corresponds to the inability of dielectric molecules to reorient themselves with an alternating gradient of the electric field. The material permittivity (ε^*) under

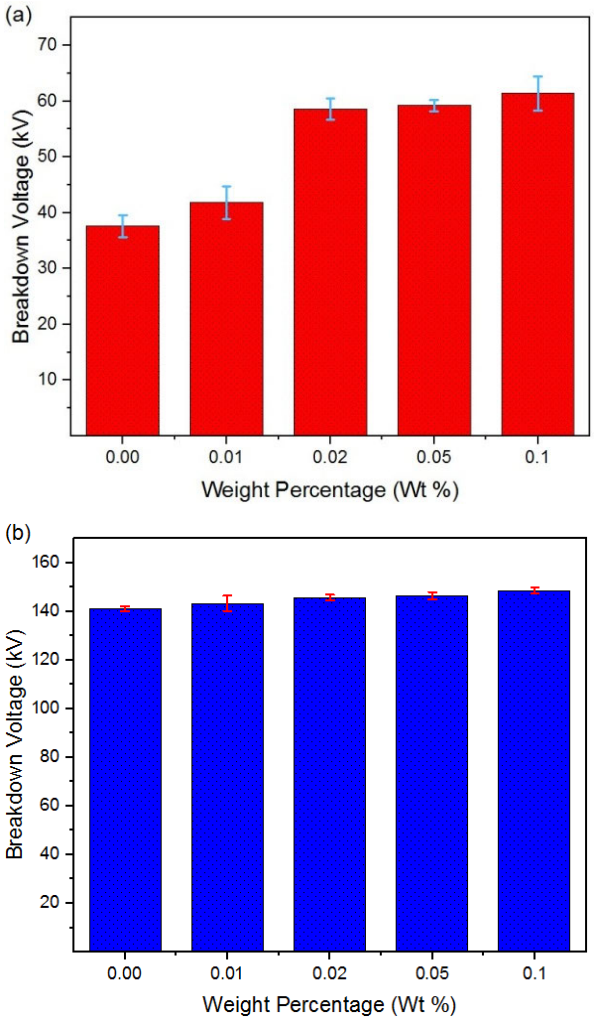

FIGURE 4. Breakdown strengths of CSO/nanofluids at different weight percentages of h-BN nanoparticles: (a) AC breakdown strength and (b) Impulse breakdown strength.

TABLE 4. AC and impulse breakdown test results.

Sample (wt %)	AC BDV			Impulse BDV		
	Mean (kV)	SD	Enh. (%)	Mean (kV)	SD	Enh. (%)
0.00	37.6	2	0	141.2	1.16	0
0.01	41.8	2.9	11.17	143.4	3.12	1.56
0.02	58.6	1.95	55.85	145.8	1.16	3.26
0.05	59.2	0.97	57.45	146.6	1.49	3.82
0.1	61.4	3.09	63.30	148.8	1.32	5.38

alternating electrical field is a complex parameter given as follows:

$$\varepsilon * = \varepsilon' - \mathrm{i}\varepsilon'' \tag{2}$$

where, ε' is the real part that gives an indication for the degree of polarization and ε'' is the imaginary part that gives an indication for the dielectric losses.

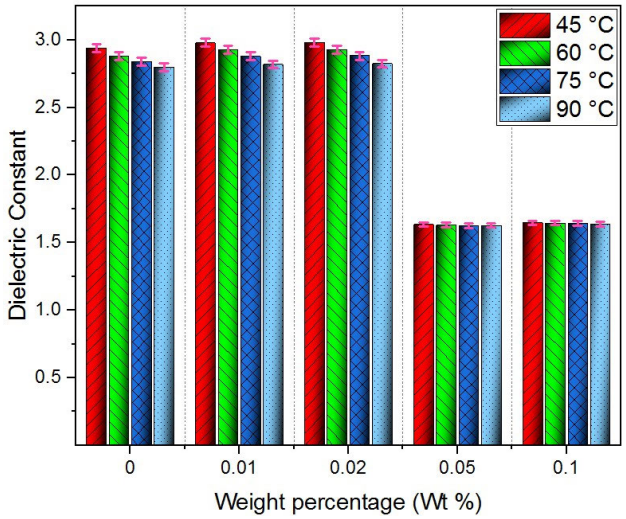

FIGURE 5. Dielectric constant variance of CSO/nanofluids at different weight percentages of h-BN nanoparticles and temperatures.

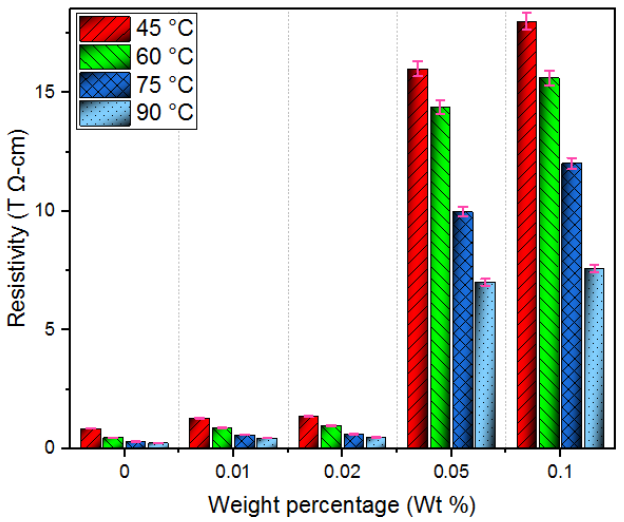

FIGURE 6. Volume resistivity of CSO/nanofluids at different weight percentages of h-BN nanoparticles and temperatures.

The dielectric constant of CSO/nanofluids is depicted in Fig. 5. The dielectric constant reduces with the increase in temperature at each weight percentage similar to that obtained in literature [23]. At 45 °C, the results indicated a small increase in the dielectric constant with the rise in the nanoparticles weight percentage up to 0.02 wt%. This increase was only about 1.3% at 0.02 wt%. Above 0.02 wt%, the dielectric constant decreased remarkably. These trends can be explained considering the expected polarization types in nanofluids as will be discussed in section 5.5.

C. VOLUME RESISTIVITY OF CSO/NANOFLUIDS

A fluid volume resistivity is a dc measurement of its electrical resistance to leakage current. Volume resistivity (Ω/cm) is the ratio of direct potential gradient (V/cm) parallel to the current density (A/cm^2) in the sample at a given time and prescribed conditions. The existence of conductive contaminants is normally indicated by a lower resistivity. Inherently, natural esters provide a smaller volume resistivity compared to mineral oils [24]. For CSO/nanofluids, volume resistivity against weight percentages of h-BN nanoparticles at various temperatures is illustrated in Fig. 6. The volume resistivity increases with filler levels from 0.0 wt% to 0.1 wt%. This improvement is attributed to the decrease in the mobility of charge carriers either due to trapping by nanoparticles or due to losing their energy by the rigid structure created at nanoparticle/oil interface. Furthermore, the decrement in volume resistivity against temperature at all weight percentages is attributed to the availability of more free charge carriers. These concepts are explained in detail in the upcoming section 5.5.

D. DISSIPATION FACTOR OF CSO/NANOFLUIDS

Dissipation factor indicates energy loss, and thus it is responsible for dielectric overheating under specific voltage, frequency, and temperature circumstances. A high dissipation

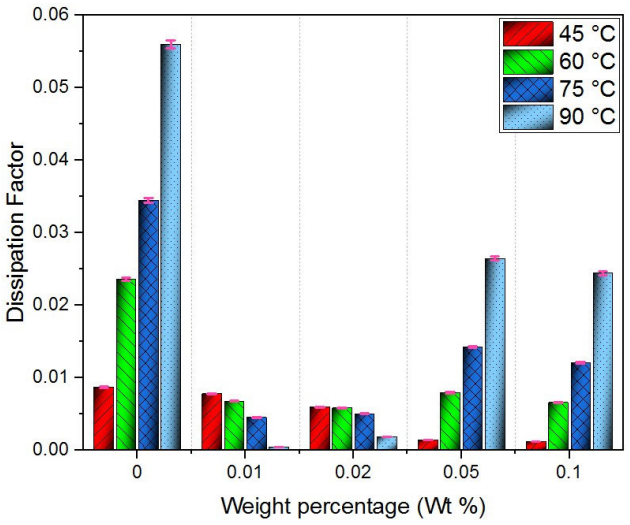

FIGURE 7. Dissipation factors of CSO/nanofluids at different weight percentages of h-BN nanoparticles and temperatures.

factor demonstrates higher dielectric losses. Losses correlated with the dissipation factor should not be confused with losses correlated with transformer loading and excitation. The losses correlated with the dissipation factor remain smaller than that for loading and excitation in several orders of magnitude. Inherently, natural esters have larger dissipation factors than mineral oils [25]. The term dissipation factor is often referred as the loss tangent and is defined as:

$$\tan\delta = \frac{\varepsilon''}{\varepsilon'} = \frac{I_l}{I_c} = \frac{\sigma_{ac}}{\omega\varepsilon'} \tag{3}$$

where, δ is the loss angle between the charging current I_c and the effective current I_l.

Fig. 7 depicts the dissipation factor of CSO/nanofluids at different weight percentages of h-BN nanoparticles with varying the temperature. According to Equation (3),

the dissipation factor is directly proportional to conductivity and inversely proportional to permittivity. There are three main results can be observed from Fig. 7 as follows. (1) At 45 °C, the dissipation factor decreases with the increase in the filler levels from 0.0 wt% to 0.1 wt%. (2) For base CSO fluid, there is a large increment in the dissipation factor with the increase in the temperature. (3) The dissipation factor decreases slightly against temperature at 0.01 wt% and 0.02 wt%, while it increases against temperature at 0.05 wt% and 0.1 wt%. The mechanisms behind these results will be discussed in the next section.

E. PHYSICAL MECHANISMS BEHIND DIELECTRIC PROPERTIES OF CSO/NANOFLUIDS

There are two different mechanisms that can be responsible for dielectric properties of CSO/nanofluids. The first mechanism is the ability of nanoparticles to trap charges, which consequently depends on dielectric relaxation time. Dielectric relaxation time is highly dependent on the permittivity (ε) and electrical conductivity (σ) of the nanoparticles, together with the surrounding fluid. The relaxation time of the nanoparticles in the fluid ($\tau_{\mathrm{h-BN}}$) is taken from Laplace equation [26] and can be represented as:

$$\tau_{\mathrm{h-BN}} = \frac{2\varepsilon_1 + \varepsilon_2}{2\sigma_1 + \sigma_2} \tag{4}$$

where, subscripts 1 and 2 denote to CSO and nanoparticles, respectively. From many literatures, the electric conductivity of CSO is apparent within the range $10^{-9} - 10^{-12}$ S.m^{-1} and its permittivity was measured $2.95\varepsilon_o$ F.m^{-1}. For h-BN nanoparticles, the value of electric conductivity is less than 10^{-13} S.m^{-1} [27], and their permittivity was found in the range of $4.0\varepsilon_o - 4.4\varepsilon_o$. With the lowest range, the relaxation time ($\tau_{\mathrm{h-BN}}$) was found to be about 43.85 ms according to Equation (4). There are four modes of streamer propagation in dielectric fluids [28]. The first and second modes occur at relatively low velocities and charges can be trapped by nanoparticles. This explains the enhancement in breakdown strength under AC voltage. However, under impulse voltage application, the third and fourth modes predominate. These modes are very fast compared to the relaxation time of nanoparticles making it difficult for nanoparticles to trap charges. Therefore, the charge trapping cannot contribute to the enhancement in impulse breakdown strength.

The second mechanism responsible for dielectric properties of CSO/nanofluids is governed by nanoparticle/oil interface. According to the theory of electrical double-layer (EDL) [29], the surface of nanoparticles in contact with transformer oil will accumulate free charges. These surface charges attract the counter-ions in the transformer oil as well as repulse the co-ions. Immediately next to the surface of the charged nanoparticles, there is a sheet of counter-ions that are highly bound to the particle surface and are immobile. This layer is known as a compact layer and has a rigid structure. From the compact layer to the electrically neutral transformer oil, a second layer called the diffuse layer is formed, through which the net charge density slowly falls to zero. Ions in the diffuse layer are mobile and are influenced easily by electrostatic forces.

EDL acts towards decreasing the energy of brisk electrons produced under high electrical field and trapping them as shown in Fig. 8. Due to the uniform distribution of nanoparticles in the oil, interfacial volumes predominate creating a lot of traps in the system. Higher concentration of nanoparticles results in greater interfacial volume, leading to more traps. This improves the insulation characteristics of oil including AC breakdown strength and volume resistivity. For impulse breakdown strength, the propagation velocity is very fast with limited time for charge trapping in EDL.

Regarding dielectric constant, it can be explained considering the expected polarization types in nanofluids. According to polarization model of oil mixtures with solid particles, there are two possible types of polarization, the polarization of oil molecules and the inner polarization of solid particles. But, with decreasing the size of solid particles to nanoscale, a third polarization is originated for oil molecules which are positioned at nanoparticle/oil interface. This third polarization has limited polarizability due to the rigid and aligned structure created at this region [30], [31]. So, the relative permittivity of CSO/nanofluids can be expressed by Clausius-Mossotti equation as follows:

$$\frac{\varepsilon - 1}{\varepsilon + 2} = \frac{1}{3\varepsilon_0}\left[(\mathrm{N}_1 - \mathrm{N}_3)\,\alpha_1 + \mathrm{N}_2\alpha_2 + \mathrm{N}_3\alpha_3\right] \tag{5}$$

At a low concentration of h-BN nanoparticles (0.01 wt% and 0.02 wt%), nanofluids have a slightly higher relative permittivity than that of pure CSO. According to Clausius-Mossotti equation, this higher relative permittivity is predominantly due to the increase in total polarization of h-BN nanoparticles due to the increase in the number of nanoparticles (N_2). On other side, at higher concentration of h-BN nanoparticles (0.05 wt% to 0.1 wt%), the amount of dispersed h-BN nanosheets per unit volume is high. This leads to an increase in the number of oil molecules at nanoparticle/oil interface (N_3) that have limited polarization with a subsequent decrease in the number of oil molecules at the free space (oil molecules other than that at nanoparticle/oil interface). As a result, the first polarization term in Equation (5) significantly decreases, while the second and third terms slightly increase. According to these key factors, the dielectric constant at 0.05 wt% and 0.1 wt% drops.

Regarding dissipation factor, it generally decreases with the increase in the weight percentages from 0.0 wt% to 0.1 wt% as obtained at 45 °C. This may be due to charge trapping by nanoparticles and EDL with a subsequent decrease in the mobility of charge carriers and the electric conductivity. For base CSO fluid, there is an increment in the dissipation factor with the increase in the temperature as usual in dielectric fluids, due to the increase of charge carriers and subsequent increase of conductivity. The temperature-dependency of dissipation factor exhibited a slight decrease against temperature at 0.01 wt% and 0.02 wt% and an increase

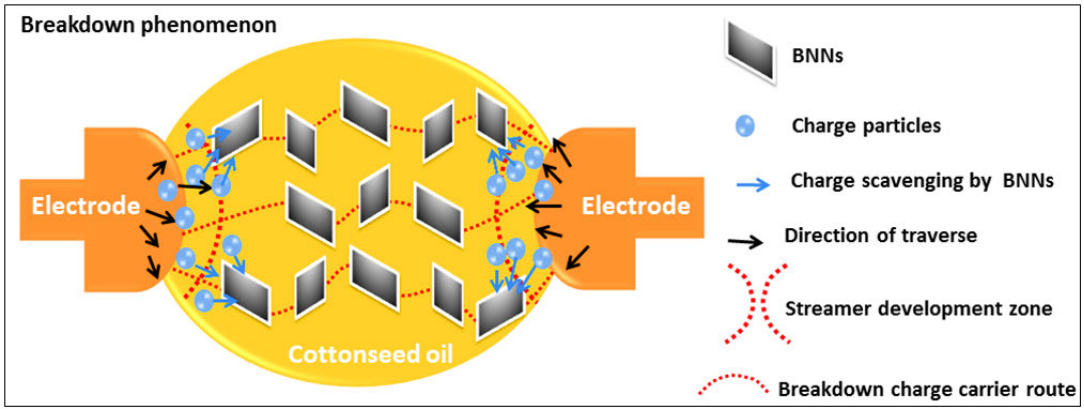

FIGURE 8. Pictorial overview of breakdown phenomena in CSO nanofluids.

against temperature at 0.05 wt% and 0.1 wt%. This trend is attributed to the effect of electrophoresis, which results in a decrease in electrical conductivity against temperature for a certain temperature range and an increase in electrical conductivity against temperature for another temperature range [32]. Under AC voltage application the h-BN nanoparticles with its EDL migrate through the fluid according to Brownian motion [33] and following the AC voltage polarity. This migration reverses each half-cycle of the applied voltage. The temperature rise in this case increases Brownian motion [33]. For small weight percentages of nanoparticles, migration of nanoparticles assists in scavenging charge carriers into the fluid, thereby decreasing the conductivity and decreasing the dissipation factor. For higher weight percentages of nanoparticles, the distance between nanoparticles decreases. Increasing Brownian motion of nanoparticles with the temperature rise allows overlaps between adjacent EDLs, and thus facilitates transport of charge carriers. This increases the conductivity with a subsequent increase in the dissipation factor.

VI. THERMAL ANALYSIS OF CSO/h-BN DISPERSED NANOFLUIDS

Cooling is the second role of transformer oil. Accordingly, the heat conductance of CSO/nanofluids has been examined in comparison to base CSO by measurement of thermal conductivity, thermal response analysis and thermal images.

A. THERMAL CONDUCTIVITY AND THERMAL RESPONSE ANALYSIS

Fig. 9a shows the thermal conductivity of CSO/nanofluids against weight percentage of h-BN nanoparticles for a temperature range between 35 °C and 65 °C. With the introduction of h-BN nanoparticles, the thermal conductivity continued to increase against weight percentage until attained about 0.221 W/m.K at 0.1 wt% and 35 °C. This represents an enhancement of 33% compared to base TBHQ CSO. The significant increase in the thermal conductivity of nanofluids deviates from the classical Maxwell theory [34].

Also, base TBHQ CSO thermal conductivity is almost flat at temperatures ranging from 35 to 65 °C and is compatible with that obtained in literature [35]. But, the thermal conductivity of nanofluids is temperature-dependent, making nanofluids act as smart fluids capable to dissipate more heat at higher temperatures. This confirm the role of h-BN nanoparticles in improving thermal conductivity.

Regarding thermal response, it is depicted in Fig. 9b. It is clear that nanofluids are heated and cooled down faster than base fluids. This effectiveness is improved with increasing the weight percentage of nanoparticles. This trend is similar to that obtained in graphene/transformer oil nanofluids [36].

There are three different mechanisms that are responsible for the obtained enhancement in thermal conductivity of nanofluids. The first mechanism is phonon transport through solid nanoparticles, which represents the governing mechanism of heat transport in solid materials. Phonon transport is originated from lattice vibrations [37]. The phonon mean free path is in the order of few tens of nm. In nanofluids, the ballistic phonon transport predominate the heat transport process as illustrated in Fig. 9c, since the size of h-BN nanoparticles reaches near the phonon mean free path. As shown in Fig. 9c, the 2D structure of h-BN creates stacks of nanosheets that produce pathways for successful heat transfer even at low weight percentages. With increasing the temperature, the atoms within the nanostructures move faster and vibrate in their mean position increasing the number of phonons.

The second mechanism is Brownian movement of nanoparticles [33]. The enhanced thermal conductivity due to Brownian movement is expressed by the following formula [38]:

$$\frac{\lambda_{nf}}{\lambda_f} = \frac{\lambda_p + 2\lambda_f + 2\varphi\left(\lambda_f + \lambda_p\right)}{\lambda_p + 2\lambda_f - \varphi\left(\lambda_f + \lambda_p\right)} + \frac{\rho_p \varphi c_p}{2\lambda_f}\left(\sqrt{\frac{k_B T}{3\Pi r \mu_{nf}}}\right) \quad (6)$$

where the second term accounts for the enhancement due to Brownian movement. It is clear that Brownian movement effect rises with increasing the temperature, giving increased thermal performance. In addition to the contribution of Brownian movement itself to the thermal conductance, it also helps transmit phonons between nanoparticles.

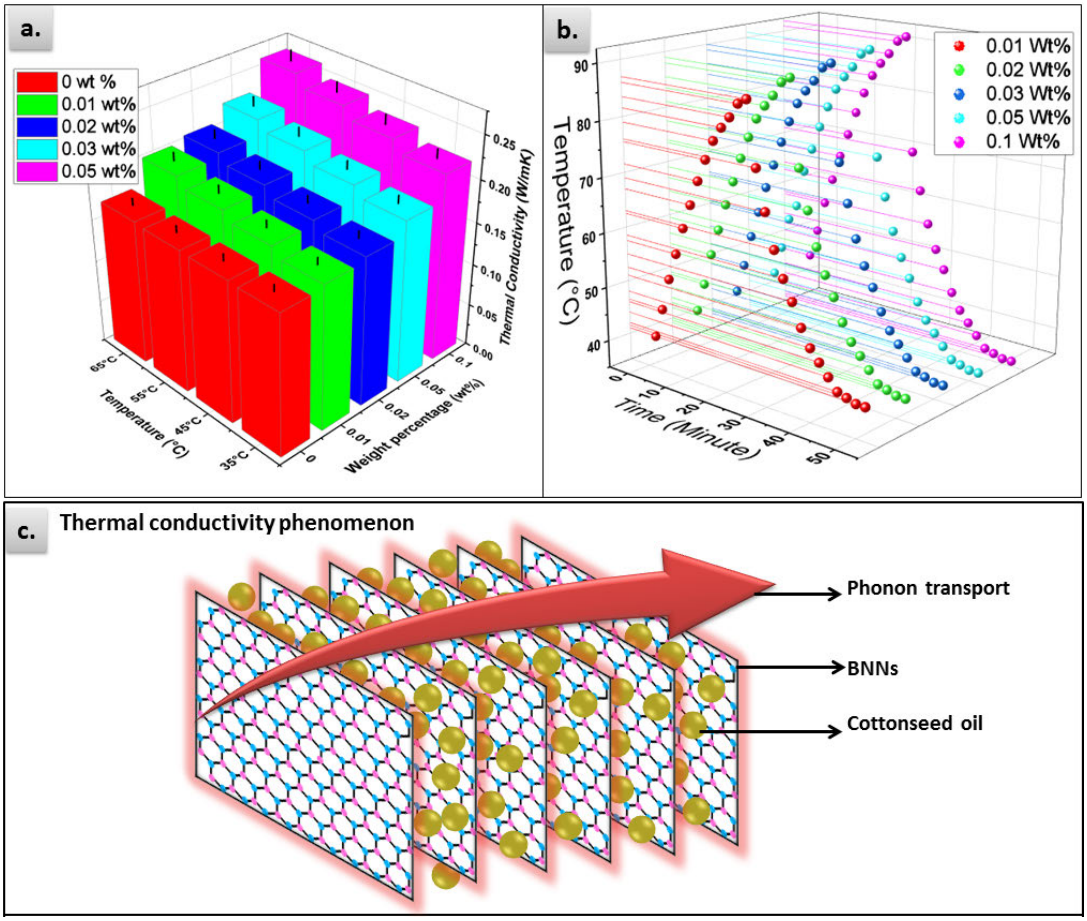

FIGURE 9. (a) Improvement of thermal conductivity of nanofluids with h-BN loading wt% and temperature (b) Nanofluid thermal response over long periods of time (c) Nanofluid heat transport mechanism.

The third mechanism that can contribute to enhanced thermal conductivity is the interparticle interactions due to the EDL at nanoparticle/oil interface [39]. This EDL causes a repulsion Coulomb force on nanoparticles resulting in an additional movement of nanoparticles with a subsequent enhancement in thermal conductivity. Also, EDL facilitates the phonon transport between adjacent nanoparticles, especially with the elevated interfacial area created by the 2D structure of h-BN nanoparticles [40].

It is important to point out that agglomeration of nanoparticles affects thermal conductivity of constituting nanofluids [41]. But, this effect is omitted in the present study, where average h-BN size observed by TEM and stability of nanofluids observed by UV-Vis spectroscopy indicated that samples are agglomerate free.

B. 6.2. THERMOGRAM ANALYSIS

The infrared optical images taken to support improved thermal conductivity in CSO/nanofluids are displayed in Fig. 10. All samples have been analyzed in the same range of temperature. The images show that the surface temperature of nanofluids at selected time period is above the base CSO and has an increasing tendency with the weight percentage. The average surface temperature recorded for base CSO and nanofluids with maximum weight percentage of 0.1 wt% were 95 °C and 104 °C, respectively, after 45 minutes of heating. This validates the better thermal conduction of nanofluids.

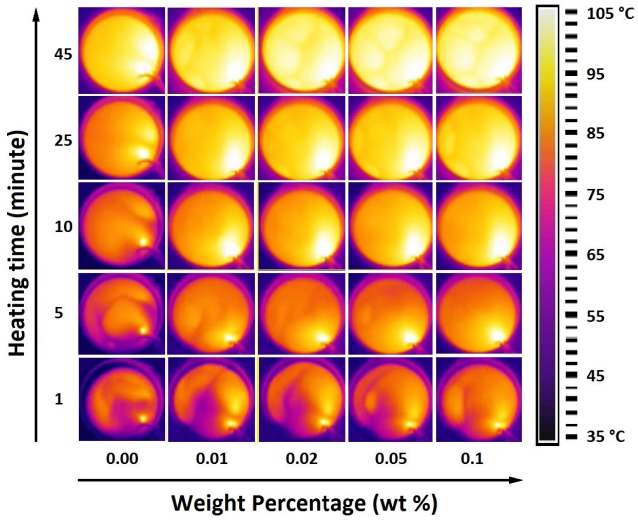

FIGURE 10. Thermogram of base CSO and nanofluids with different heating times and weight percentages.

VII. CONCLUSION

In this article, non-edible cottonseed oil (CSO) was developed as natural ester insulating fluids through inclusion of antioxidant and filling with h-BN nanofillers. Different weight percentages of h-BN nanoparticles have been used ranging from 0.01 wt% to 0.1 wt%. The dispersion of nanoparticles and their suspension stability have been confirmed through TEM observation and UV-Vis spectroscopy. The usage of h-BN nanoparticles could simultaneously improve dielectric and thermal properties as follows:

1. An enhancement in AC breakdown voltage was achieved and attained a maximum percentage increment of 63.3% at a weight percentage of 0.1 wt%. On the other hand, impulse breakdown voltage has been enhanced to a little extent of about 5%. These results were explained considering the charge trapping by nanoparticles themselves or by EDL created at nanoparticle/oil interface.
2. The dielectric constant of CSO/nanofluids indicated a small increase with the weight percentage of nanoparticles up to 0.02 wt%, and then a remarkable decrease above 0.02 wt%. These trends were explained considering the different polarization types in nanofluids.
3. The volume resistivity of nanofluids increased and their dissipation factor decreased against weight percentages of h-BN nanoparticles due to the charge trapping effect.
4. The thermal conductivity of nanofluids enhanced significantly compared to base CSO as validated from thermal conductivity measurement, thermal response analysis, and thermogram analysis. Also, the thermal conductivity of nanofluids was temperature-dependent capable to dissipate more heat at higher temperatures. These enhancements have been explained considering phonon transport through nanoparticles, their Brownian movement, and interparticle interactions due to the EDL at nanoparticle/oil interface.

All the obtained results and clarified mechanisms in the present study validate the superiority of CSO based h-BN nanofluids as a potential candidate either for power equipment or for management systems of thermal energy.

REFERENCES

[1] G. M. Turky and R. A. El-Adly, "Study of phase separation and anomalous molecular behavior of jojoba oil using dielectric spectroscopy," *J. Mol. Liquids*, vol. 242, pp. 1–7, Sep. 2017.

[2] S. R. Valantina, K. A. Jayalatha, D. R. P. Angeline, S. Uma, and B. Ashvanth, "Synthesis and characterisation of electro-rheological property of novel eco-friendly rice bran oil and nanofluid," *J. Mol. Liquids*, vol. 256, pp. 256–266, Apr. 2018.

[3] M. M. M. Salama, D.-E.-A. Mansour, M. Daghrah, S. M. Abdelkasoud, and A. A. Abbas, "Thermal performance of transformers filled with environmentally friendly oils under various loading conditions," *Int. J. Electr. Power Energy Syst.*, vol. 118, Jun. 2020, Art. no. 105743.

[4] S. Singha, R. Asano, G. Frimpong, C. C. Claiborne, and D. Cherry, "Comparative aging characteristics between a high oleic natural ester dielectric liquid and mineral oil," *IEEE Trans. Dielectr. Electr. Insul.*, vol. 21, no. 1, pp. 149–158, Feb. 2014.

[5] *COTTON 2020 Roadmap for Sustainable Production*, Fed. Indian Chambers Commerce Ind., New Delhi, India, 2012.

[6] A. Raymon, S. Sakthibalan, C. Cinthal, R. Subramaniaraja, and M. Yuvaraj, "Enhancement and comparison of nano-ester insulating fluids," *IEEE Trans. Dielectr. Electr. Insul.*, vol. 23, no. 2, pp. 892–900, Apr. 2016.

[7] Q. Liu, S. P. Singh, and A. G. Green, "High-stearic and high-oleic cottonseed oils produced by hairpin RNA-mediated post-transcriptional gene silencing," *Plant Physiol.*, vol. 129, no. 4, pp. 1732–1743, Aug. 2002.

[8] M. M. Emara, D.-E.-A. Mansour, and A. M. Azmy, "Mitigating the impact of aging byproducts in transformer oil using TiO_2 nanofillers," *IEEE Trans. Dielectr. Electr. Insul.*, vol. 24, no. 6, pp. 3471–3480, Dec. 2017.

[9] M. E. M. Soudagar, N.-N. Nik-Ghazali, M. A. Kalam, I. A. Badruddin, N. R. Banapurmath, and N. Akram, "The effect of nano-additives in diesel-biodiesel fuel blends: A comprehensive review on stability, engine performance and emission characteristics," *Energy Convers. Manage.*, vol. 178, pp. 146–177, Dec. 2018.

[10] U. Khaled and A. Beroual, "Statistical investigation of AC dielectric strength of natural ester oil-based Fe_3O_4, Al_2O_3, and SiO_2 nano-fluids," *IEEE Access*, vol. 7, pp. 60594–60601, 2019.

[11] M. E. M. Soudagar, N.-N. Nik-Ghazali, M. A. Kalam, I. A. Badruddin, N. R. Banapurmath, T. M. Yunus Khan, M. N. Bashir, N. Akram, R. Farade, and A. Afzal, "The effects of graphene oxide nanoparticle additive stably dispersed in dairy scum oil biodiesel-diesel fuel blend on CI engine: Performance, emission and combustion characteristics," *Fuel*, vol. 257, Dec. 2019, Art. no. 116015.

[12] D.-E.-A. Mansour, E. M. Shaalan, S. A. Ward, A. Z. El Dein, H. S. Karaman, and H. M. Ahmed, "Multiple nanoparticles for improvement of thermal and dielectric properties of oil nanofluids," *IET Sci., Meas. Technol.*, vol. 13, no. 7, pp. 968–974, Sep. 2019.

[13] R. Madavan, S. S. Kumar, and M. W. Iruthyarajan, "A comparative investigation on effects of nanoparticles on characteristics of natural esters-based nanofluids," *Colloids Surf. A, Physicochem. Eng. Aspects*, vol. 556, pp. 30–36, Nov. 2018.

[14] W. Yao, Z. Huang, J. Li, L. Wu, and C. Xiang, "Enhanced electrical insulation and heat transfer performance of vegetable oil based nanofluids," *J. Nanomater.*, vol. 2018, Apr. 2018, Art. no. 4504208.

[15] J. Taha-Tijerina, T. N. Narayanan, G. Gao, M. Rohde, D. A. Tsentalovich, M. Pasquali, and P. M. Ajayan, "Electrically insulating thermal nano-oils using 2D fillers," *ACS Nano*, vol. 6, no. 2, pp. 1214–1220, Feb. 2012.

[16] J. Li, Z. Zhang, P. Zou, S. Grzybowski, and M. Zahn, "Preparation of a vegetable oil-based nanofluid and investigation of its breakdown and dielectric properties," *IEEE Elect. Insul. Mag.*, vol. 28, no. 5, pp. 43–50, Sep. 2012.

[17] J. Li, B. Du, F. Wang, W. Yao, and S. Yao, "The effect of nanoparticle surfactant polarization on trapping depth of vegetable insulating oil-based nanofluids," *Phys. Lett. A*, vol. 380, no. 4, pp. 604–608, Feb. 2016.

[18] M. Javed, A. H. Shaik, T. A. Khan, M. Imran, A. Aziz, A. R. Ansari, and M. R. Chandan, "Synthesis of stable waste palm oil based CuO nanofluid for heat transfer applications," *Heat Mass Transf.*, vol. 54, no. 12, pp. 3739–3745, Dec. 2018.

[19] A. Hameed, A. Mukhtar, U. Shafiq, M. Qizilbash, M. S. Khan, T. Rashid, C. B. Bavoh, W. U. Rehman, and A. Guardo, "Experimental investigation on synthesis, characterization, stability, thermo-physical properties and rheological behavior of MWCNTs-kapok seed oil based nanofluid," *J. Mol. Liquids*, vol. 277, pp. 812–824, Mar. 2019.

[20] Z. Hu, S. Wang, G. Chen, Q. Zhang, K. Wu, J. Shi, L. Liang, and M. Lu, "An aqueous-only, green route to exfoliate boron nitride for preparation of high thermal conductive boron nitride nanosheet/cellulose nanofiber flexible film," *Composites Sci. Technol.*, vol. 168, pp. 287–295, Nov. 2018.

[21] N. Yang, C. Xu, J. Hou, Y. Yao, Q. Zhang, M. E. Grami, L. He, N. Wang, and X. Qu, "Preparation and properties of thermally conductive polyimide/boron nitride composites," *RSC Adv.*, vol. 6, no. 22, pp. 18279–18287, 2016.

[22] R. N. Muthu, S. Rajashabala, and R. Kannan, "Hydrogen storage performance of lithium borohydride decorated activated hexagonal boron nitride nanocomposite for fuel cell applications," *Int. J. Hydrogen Energy*, vol. 42, no. 23, pp. 15586–15596, Jun. 2017.

[23] M. H. A. Hamid, M. T. Ishak, M. F. M. Din, N. S. Suhaimi, and N. I. A. Katim, "Dielectric properties of natural ester oils used for transformer application under temperature variation," in *Proc. IEEE Int. Conf. Power Energy (PECon)*, Melaka, Malaysia, Nov. 2016, pp. 54–57.

[24] S. Arazoe, D. Saruhashi, Y. Sato, S. Yanabu, G. Ueta, and S. Okabe, "Electrical characteristics of natural and synthetic insulating fluids," *IEEE Trans. Dielectr. Electr. Insul.*, vol. 18, no. 2, pp. 506–512, Apr. 2011.

[25] *IEEE Guide for Acceptance and Maintenance of Natural Ester Insulating Liquid in Transformers*, IEEE Standard C57.147-2018, 2018.
[26] J. G. Hwang, M. Zahn, F. M. O'Sullivan, L. A. A. Pettersson, O. Hjortstam, and R. Liu, "Effects of nanoparticle charging on streamer development in transformer oil-based nanofluids," *J. Appl. Phys.*, vol. 107, no. 1, Jan. 2010, Art. no. 014310.
[27] C. Steinborn, M. Herrmann, U. Keitel, A. Schönecker, J. Räthel, D. Rafaja, and J. Eichler, "Correlation between microstructure and electrical resistivity of hexagonal boron nitride ceramics," *J. Eur. Ceram. Soc.*, vol. 33, no. 6, pp. 1225–1235, Jun. 2013.
[28] O. Lesaint and G. Massala, "Positive streamer propagation in large oil gaps: Experimental characterization of propagation modes," *IEEE Trans. Dielectr. Electr. Insul.*, vol. 5, no. 3, pp. 360–370, Jun. 1998.
[29] N. Ise and I. S. Sogami, *Structure Formation in Solution: Ionic Polymers and Colloidal Particles*. New York, NY, USA: Springer-Verlag, 2005.
[30] R. Kochetov, T. Andritsch, P. H. F. Morshuis, and J. J. Smit, "Anomalous behaviour of the dielectric spectroscopy response of nanocomposites," *IEEE Trans. Dielectr. Electr. Insul.*, vol. 19, no. 1, pp. 107–117, Feb. 2012.
[31] D.-E.-A. Mansour, A. M. Elsaeed, and M. A. Izzularab, "The role of interfacial zone in dielectric properties of transformer oil-based nanofluids," *IEEE Trans. Dielectr. Electr. Insul.*, vol. 23, no. 6, pp. 3364–3372, Dec. 2016.
[32] M. Dong, L. P. Shen, H. Wang, H. B. Wang, and J. Miao, "Investigation on the electrical conductivity of transformer oil-based AlN nanofluid," *J. Nanomater.*, vol. 2013, Dec. 2013, Art. no. 842963.
[33] S. P. Jang and S. U. S. Choi, "Role of Brownian motion in the enhanced thermal conductivity of nanofluids," *Appl. Phys. Lett.*, vol. 84, no. 21, pp. 4316–4318, May 2004.
[34] S. Mehta, K. P. Chauhan, and S. Kanagaraj, "Modeling of thermal conductivity of nanofluids by modifying Maxwell's equation using cell model approach," *J. Nanopart. Res.*, vol. 13, no. 7, pp. 2791–2798, Jul. 2011.
[35] E. E. G. Rojas, J. S. R. Coimbra, and J. Telis-Romero, "Thermophysical properties of cotton, canola, sunflower and soybean oils as a function of temperature," *Int. J. Food Properties*, vol. 16, no. 7, pp. 1620–1629, Oct. 2013.
[36] M. M. Bhunia, K. Panigrahi, S. Das, K. K. Chattopadhyay, and P. Chattopadhyay, "Amorphous graphene—Transformer oil nanofluids with superior thermal and insulating properties," *Carbon*, vol. 139, pp. 1010–1019, Nov. 2018.
[37] A. M. Hofmeister, *Measurements, Mechanisms, and Models of Heat Transport*, 1st ed. Amsterdam, The Netherlands: Elsevier, 2019.
[38] J.-M. Liu, Z.-H. Liu, and Y.-J. Chen, "Experiment and calculation of the thermal conductivity of nanofluid under electric field," *Int. J. Heat Mass Transf.*, vol. 107, pp. 6–12, Apr. 2017.
[39] J.-Y. Jung and J. Y. Yoo, "Thermal conductivity enhancement of nanofluids in conjunction with electrical double layer (EDL)," *Int. J. Heat Mass Transf.*, vol. 52, nos. 1–2, pp. 525–528, Jan. 2009.
[40] D. Lee, "Thermophysical properties of interfacial layer in nanofluids," *Langmuir*, vol. 23, no. 11, pp. 6011–6018, May 2007.
[41] M. R. Rodríguez-Laguna, A. Castro-Alvarez, M. Sledzinska, J. Maire, F. Costanzo, B. Ensing, M. Pruneda, P. Ordejón, C. M. S. Torres, P. Gómez-Romero, and E. Chávez-Ángel, "Mechanisms behind the enhancement of thermal properties of graphene nanofluids," *Nanoscale*, vol. 10, no. 32, pp. 15402–15409, 2018.

RIZWAN A. FARADE received the B.E. degree in electrical and electronics engineering from Visvesvaraya Technological University, Belgaum, India, in 2005, and the M.Tech degree in power electronics from Jawaharlal Nehru Technological University, Hyderabad, India, in 2013. He is currently pursuing the Ph.D. degree in electrical and electronics engineering with University Putra Malaysia, Serdang, Malaysia. Since 2009, he has been a Lecturer and an Assistant Professor in India's diploma and undergraduate programs. Since 2014, he has also been with Kalsekar Technical Campus, New Mumbai, India, as an Assistant Professor in undergraduate program. His research interests include dielectric fluids, power systems, and nano biodiesel.

NOOR IZZRI BIN ABDUL WAHAB (Senior Member, IEEE) received the degree in electrical and electronic engineering from the University of Manchester Institute of Science and Technology (UMIST), U.K., in 1998, the M.Sc. degree in electrical power engineering from Universiti Putra Malaysia (UPM), in 2002, and the Ph.D. degree in electrical, electronic, and system engineering from Universiti Kebangsaan Malaysia (UKM), in 2010. He is currently an Associate Professor with the Department of Electrical and Electronic Engineering, Faculty of Engineering, UPM. He is also the Founding Member of the Advanced Lightning, Power and Energy Research Centre (ALPER), UPM. He is also a Registered Chartered Engineer (CEng), a Professional Engineer (Ir.), a Member of The Institution of Engineers Malaysia (IEM). His areas of interest include power system stability, application of AI in power systems, and power quality.

DIAA-ELDIN A. MANSOUR (Senior Member, IEEE) was born in Tanta, Egypt, in December 1978. He received the B.Sc. and M.Sc. degrees in electrical engineering from Tanta University, Tanta, Egypt, in 2000 and 2004, respectively, and the Ph.D. degree in electrical engineering from Nagoya University, Nagoya, Japan, in 2010. Since 2000, he has been with the Department of Electrical Power and Machines Engineering, Faculty of Engineering, Tanta University, Egypt, working as an Instructor, an Assistant Lecturer, and currently, an Assistant Professor and the Director of High Voltage and Superconductivity Laboratory. In 2010, he was a Foreign Researcher for three months at EcoTopia Science Institute, Nagoya University, Nagoya, Japan. His research interests are high voltage engineering, condition monitoring and diagnosis of electrical power equipment, nanodielectrics, and applied superconductivity. He received the best presentation award two times from IEE of Japan, in 2008 and 2009. His Prize from the Egyptian Academy of Scientific Research and Technology, in 2013, the Tanta University Encouragement Award, in 2017, and the State Encouragement Award, in 2018.

NORHAFIZ B. AZIS (Senior Member, IEEE) received B.Eng. degree in electrical and electronic engineering from Universiti Putra Malaysia, in 2007, and the Ph.D. degree in electrical power engineering from The University of Manchester, U.K., in 2012. He is currently an Associate Professor with the Department of Electrical and Electronic Engineering, Universiti Putra Malaysia, Malaysia. His research interests are in-service ageing of transformer insulation, condition monitoring, and asset management and alternative insulation materials for transformers.

JASRONITA JASNI (Senior Member, IEEE) received the B.Eng. and M.Eng. degrees in electrical engineering from Universiti Teknologi Malaysia, Johor, Malaysia, in 1998 and 2001, respectively, and the Ph.D. degree in electrical power engineering from Universiti Putra Malaysia, Selangor, Malaysia, in 2010. From 1998 to 1999, she was a System Engineer and later from 1999 to 2001, she worked as a Tutor with the Department of Electrical and Electronics Engineering, Faculty of Engineering, Universiti Putra Malaysia. Then, in 2001, she started working as a Lecturer with the Department of Electrical and Electronics Engineering, Universiti Putra Malaysia. She is currently an Associate Professor with the Department of Electrical and Electronics Engineering, Faculty of Engineering, Universiti Putra Malaysia. Her research interests include power systems, renewable energy, and lightning protection. She received several awards and recognitions for her work and researches, including Excellent in Service Award (Universiti Putra Malaysia), Excellent in Teaching Award (Universiti Putra Malaysia), and Bronze Medal in Malaysia Technology Expo.

N. R. BANAPURMATH received the bachelor's degree in mechanical engineering, the master's degree in heat power engineering from the National Institute of Technology Karnataka (NITK), Surathkal, and the Doctor of Philosophy degree in mechanical engineering from Visvesvaraya Technological University (VTU). He is currently working as a Professor with the School of Mechanical Engineering, B.V. Bhoomaraddi College of Engineering and Technology, and a Professor and the Head with the Centre for Material Science (CMS), K.L.E. Technological University (Previously known as the B.V. Bhoomaraddi College of Engineering and Technology) Hubballi. He has 26 years of Teaching experience and 10 years of Research, published International Journals: 169, International conference: 82, National conference: 23, Patents (filed):09, 13 Book and Book chapter publications. Several funded projects from State and Central Government of India. Guided Ph.D.:11, guided M.Tech.:30. He is a reviewer for many national and international journals.

MANZOORE ELAHI M. SOUDAGAR was born in Dharwad, India, in 1988. He received the B.Tech. and M.Tech. degrees in mechanical engineering from Visvesvaraya Technological University (VTU), Karnataka, in 2010 and 2012, respectively. He is currently pursuing the Ph.D. degree in the biodiesel production from non-edible feedstocks and effects of nano-additives on the performance and emission characteristics of diesel-biodiesel fuel, Department of Mechanical Engineering, University of Malaya, Kuala Lumpur, Malaysia. His other research interests include biodiesel production technologies, finite element analysis of porous cavities, and solar energy.